BNL-103673-2014-TECH

AGS/RHIC/SN 047;BNL-103673-2014-IR

Analytical Field Calculation of the Slotted Helical Dipole

T. Tominaka

November 1996

Collider Accelerator Department

Brookhaven National Laboratory

U.S. Department of Energy

USDOE Office of Science (SC)

DISCLAIMER

Alternating Gradient Synchrotron Department
Relativistic Heavy Ion Collider Project
BROOKHAVEN NATIONAL LABORATORY
Upton, New York 11973

Spin Note

AGS/RHIC/SN No. 047

Analytical Field Calculation of the Slotted Helical Dipole

T. Tominaka

November 12, 1996

Analytical Field Calculation of the Slotted Helical Dipole

T. Tominaka (RIKEN, Japan)

1. Introduction

The magnetic field of the slotted helical dipole designed and fabricated at the Magnet Division of BNL is calculated analytically in this paper. A schematic view of this superconducting helical dipole is given in Fig.1 The purpose of this paper is to obtain the contents of multipoles expected for the slotted helical dipole. The relation between helical multipoles and 2-dimensional multipoles is also presented. In addition, this analytical calculation is compared with the numerical calculation with the 3-dimensional magnetic field calculation code, OPERA-3d/TOSCA. [1]

2. Magnetic Field of a Originally Optimized Helical Dipole Magnet

According to the method described in Appendix, the magnetic field of a helical dipole magnet optimized by R. Gupta at BNL can be calculated analytically with the assumption of the infinite length. A quarter of the cross section of this optimized slotted helical dipole magnet is shown in Fig.2. Each black dot corresponds to a superconducting strand used as a conductor. The summation in Eq.(A3) is made for all 864 sets of four helical line currents with dipole symmetry. For the comparison, the analytically calculated contents of multipole expected for this helical dipole together with the 2-dimensional multipole coefficients for the reference radius $r0 = 30$ mm, are shown in Table 1 for the case without iron yoke and in Table 2 for the case with iron yoke. In this calculation, the effect of the iron yoke is calculated with the method of image currents, with the assumption of the helical image current similar to the straight image current. The relative permeability of iron yoke with the inner diameter of 168.9 mm (= 6.651 inches) is assumed to be infinite, and the current of conductor in the white region shown in Fig.2 is different from that in the gray region,

Current #1 (white region) : $I_1 = 290$ A,
Current #2 (gray region) : $I_2 = 290\ \text{A} \times 11/9 = 354.4$ A.

The reference field $B_{ref}(k)$, and helical multipole coefficients, $b_n(k)$ (=b-helix), of the 3-dimensional helical dipole listed in Table 1 and 2 correspond to those of Eq.(A1). On the other hand, the reference field B_{ref}, and 2-dimensional multipole coefficients, b_n (=b-2d), of the 2-dimensional dipole listed in Table 1 and 2 correspond to those of Eq.(A5). Therefore, it can be thought that the twisting from the 2-dimensional dipole to the helical dipole has mathematically two effects of changing the character of the function describing the field, and changing the values of multipoles determined by the current and position of the conductor.

3. Magnetic Field of a Actual Helical Dipole Magnet

The helical dipole magnet fabricated actually is deformed from the above-mentioned optimized one for the ease of machining. The magnetic field of this magnet slightly deformed is also calculated analytically. The cross section of this slotted helical dipole magnet is shown in Fig.3. The dimensions of this cross section are obtained from the design sheets written in BNL.

In the case without iron yoke, the contents of multipole expected for this helical dipole together with the 2-dimensional multipole coefficients for the reference radius $r0 = 30$ mm, are also shown in Table 3. The twist (or k) dependence of the reference field $B_{ref}(k)$, and the helical sextupole coefficient, $b3(k)$, are shown in Figs.4 and 5, respectively. The expressions of the radial magnetic field B_r, the azimuthal magnetic field $B\theta$, and the y-directional magnetic field B_y on the circle of radius $r = 30$ mm can be derived from Eq.(A1) with the helical multipoles shown in Table 3 as follows,

$$B_r(r=30\text{ mm}, \theta, z=0) = 2.794\,(\sin[\theta] - 19.3\ 10^{-4}\sin[3\,\theta] + 2.8\ 10^{-4}\sin[5\,\theta] - 0.095\ 10^{-4}\sin[7\,\theta] - 8.5\ 10^{-4}\sin[9\,\theta] + 3.2\ 10^{-4}\sin[11\,\theta] + 0.16\ 10^{-4}\sin[13\,\theta] - 0.36\ 10^{-4}\sin[15\,\theta] + 0.048\ 10^{-4}\sin[17\,\theta] + 0.030\ 10^{-4}\sin[19\,\theta]) \quad (1)$$

$$B_\theta(r=30\text{ mm}, \theta, z=0) = 2.789\,(\cos[\theta] - 19.3\ 10^{-4}\cos[3\,\theta] + 2.8\ 10^{-4}\cos[5\,\theta] - 0.095\ 10^{-4}\cos[7\,\theta] - 8.5\ 10^{-4}\cos[9\,\theta] + 3.2\ 10^{-4}\cos[11\,\theta] + 0.16\ 10^{-4}\cos[13\,\theta] - 0.36\ 10^{-4}\cos[15\,\theta] + 0.048\ 10^{-4}\cos[17\,\theta] + 0.029\ 10^{-4}\cos[19\,\theta]) \quad (2)$$

$$B_y(r=30\text{ mm}, \theta, z=0) = 2.792\,(1 - 27.0\ 10^{-4}\cos[2\,\theta] + 2.9\ 10^{-4}\cos[4\,\theta] - 0.099\ 10^{-4}\cos[6\,\theta] - 8.5\ 10^{-4}\cos[8\,\theta] + 3.2\ 10^{-4}\cos[10\,\theta] + 0.16\ 10^{-4}\cos[12\,\theta] - 0.36\ 10^{-4}\cos[14\,\theta] + 0.048\ 10^{-4}\cos[16\ \text{theta}] + 0.029\ 10^{-4}\cos[18\,\theta]) \quad (3)$$

These expressions are the same forms with Eq.(A5) or Eq.(A7). On the other hand, the 2-dimensional multipole coefficients can also be derived from the y component of magnetic field By on the x-axis as shown in Fig.6 by fitting. The expression is the same following form with Eq.(A8),

$$B_y(r=x, \theta=0, z=0) = 2.787\left(1. - 11.5\ 10^{-4}\left(\frac{x}{r_0}\right)^2 + 2.8\ 10^{-4}\left(\frac{x}{r_0}\right)^4 - 0.076\ 10^{-4}\left(\frac{x}{r_0}\right)^6 - 8.4\ 10^{-4}\left(\frac{x}{r_0}\right)^8 + 3.0\ 10^{-4}\left(\frac{x}{r_0}\right)^{10} + 0.20\ 10^{-4}\left(\frac{x}{r_0}\right)^{12} - 0.34\ 10^{-4}\left(\frac{x}{r_0}\right)^{14} + 0.030\ 10^{-4}\left(\frac{x}{r_0}\right)^{16} + 0.034\ 10^{-4}\left(\frac{x}{r_0}\right)^{18}\right) \quad (4)$$

From the comparison between Eq.(3) and (4), the 2-dimensional sextupole coefficients $b_3 = -11.5\ 10^{-4}$ derived from the field distribution of By on x-axis is especially different from $b_3 = -27.0\ 10^{-4}$ derived from the field distribution on the circle. This means that 2-dimensional multipole coefficients are not exactly applicable for helical dipole. The field distribution of By in the central region is shown in Fig.7, on the style of the 3-dimensional plot.

Similarly, in the case with iron yoke, the contents of multipole expected for this helical dipole together with the 2-dimensional multipole coefficients for the reference radius $r_0 = 30$ mm, are also shown in Table 4. The expressions of the radial magnetic field B_r, the azimuthal magnetic field B_θ, and the y component of magnetic field By on the circle of radius r= 30 mm, and the y component of magnetic field By on the x-axis are as follows,

$$B_r(r=30\text{ mm}, \theta, z=0) = 4.513\,(\sin[\theta] - 2.5\ 10^{-4}\sin[3\,\theta] + 0.55\ 10^{-4}\sin[5\,\theta] - 0.14\ 10^{-4}\sin[7\,\theta] - 5.3\ 10^{-4}\sin[9\,\theta] + 2.0\ 10^{-4}\sin[11\,\theta] + 0.10\ 10^{-4}\sin[13\,\theta] - 0.23\ 10^{-4}\sin[15\,\theta] + 0.030\ 10^{-4}\sin[17\,\theta] + 0.018\ 10^{-4}\sin[19\,\theta]) \quad (5)$$

$$B_\theta(r=30\text{ mm}, \theta, z=0) = 4.506\,(\cos[\theta] - 2.5\ 10^{-4}\cos[3\,\theta] + 0.55\ 10^{-4}\cos[5\,\theta] - 0.14\ 10^{-4}\cos[7\,\theta] - 5.3\ 10^{-4}\cos[9\,\theta] + 2.0\ 10^{-4}\cos[11\,\theta] + 0.10\ 10^{-4}\cos[13\,\theta] - 0.23\ 10^{-4}\cos[15\,\theta] + 0.029\ 10^{-4}\cos[17\,\theta] + 0.018\ 10^{-4}\cos[19\,\theta]) \quad (6)$$

$$B_y(r=30\text{ mm}, \theta, z=0) = 4.510\,(1 - 10.2\ 10^{-4}\cos[2\,\theta] + 0.55\ 10^{-4}\cos[4\,\theta] - 0.14\ 10^{-4}\cos[6\,\theta] - 5.3\ 10^{-4}\cos[8\,\theta] + 2.0\ 10^{-4}\cos[10\,\theta] + 0.098\ 10^{-4}\cos[12\,\theta] - 0.23\ 10^{-4}\cos[14\,\theta] + 0.030\ 10^{-4}\cos[16\ \text{theta}] + 0.018\ 10^{-4}\cos[18\,\theta]) \quad (7)$$

$$B_y(r=x, \theta=0, z=0) = 4.503\left(1. + 5.2\ 10^{-4}\left(\frac{x}{r_0}\right)^2 + 0.54\ 10^{-4}\left(\frac{x}{r_0}\right)^4 - 0.13\ 10^{-4}\left(\frac{x}{r_0}\right)^6 - 5.2\ 10^{-4}\left(\frac{x}{r_0}\right)^8 + 1.9\ 10^{-4}\left(\frac{x}{r_0}\right)^{10} + 0.12\ 10^{-4}\left(\frac{x}{r_0}\right)^{12} - 0.21\ 10^{-4}\left(\frac{x}{r_0}\right)^{14} + 0.019\ 10^{-4}\left(\frac{x}{r_0}\right)^{16} + 0.021\ 10^{-4}\left(\frac{x}{r_0}\right)^{18}\right) \quad (8)$$

The field distribution of By in the central region is shown in Fig.8.

4. Comparison Between Analytical and Numerical Calculation

The field of the helical dipole magnet can be numerically calculated with the 3-dimensional magnetic field calculation code, OPERA-3d/TOSCA. The cross section derived from the input data of the conductor for the OPERA-3d/TOSCA, prepared by M. Okamura is shown in Fig.9. This cross section is slightly different from that shown in Fig.3.

In the case without iron yoke, the contents of multipole expected for this helical dipole together with the 2-dimensional multipole coefficients for the reference radius r0 = 30 mm, are shown in Table 5. These values are almost same with those shown in Table 3. Similarly, the helical multipole coefficients derived form the radial magnetic field B_r, the azimuthal magnetic field B_θ, and the z component of magnetic field B_z at the center z=0 of helical coil, calculated with OPERA-3d are also shown in Table 6. From the comparison between Tables 5 and 6, it seems that the analytically obtained results are almost consistent with those obtained with the 3-dimensional magnetic field calculation code, OPERA-3d. The difference may come mainly from the difference of the length of the helical dipole. The analytical calculation assumes that the length of the helical dipole is infinite, but the field calculation with OPERA-3d is made for the actual helical dipole of the finite length with coil ends shown in Fig.1. In the case without iron yoke, the field distribution of By at z=0 calculated with OPERA-3d is shown in Fig.10.

5. Conclusion

The contents of multipole expected for the slotted helical dipole are obtained analytically, with the comparison between helical multipoles and 2-dimensional multipoles. The analytical results are almost consistent with those obtained with the 3-dimensional magnetic field calculation code, OPERA-3d. This analytical method may be also useful for the estimation of the effect of the geometrical distortion due to the twist on the multipoles of the dipole. In addition, the confusion should be avoided among the various multipoles with different definition, (1) the conventional multipole coefficients for the 2-dimensional dipole of the same cross section with the 3-dimensional helical dipole, (2) the 2-dimensional multipole coefficients for the 3-dimensional helical dipole, and (3) the helical multipole coefficients for the 3-dimensional helical dipole. From the viewpoint of the field analysis, it seems that the helical multipole coefficients naturally extended from the conventional ones are most reasonable for helical dipoles.

6. Acknowledgments

Special thanks go to the Magnet Division of BNL for providing us with a wealth of information on the RHIC helical dipole magnets. The author is also indebted for helpful discussions and comments to Prof. T. Katayama of Institute of Nuclear Physics, University of Tokyo and RIKEN and for providing me the input data of helical coil for OPERA-3d to Dr. M. Okamura of BNL/RIKEN.

Appendix 1. Magnetic Field of 3-dimensional Helical Dipole Coils

The interior magnetic field of helical dipole coil with the infinite length is as follows, [2]

$$\begin{cases} B_r(r,\theta,z) = -\dfrac{\partial \phi_h}{\partial r} = B_{ref}(k)\, r_0 \displaystyle\sum_{n=1}^{\infty} n! \left[\frac{2}{n\,k\,r_0}\right]^n k\, I_n'(n\,k\,r) \left\{-a_n(k)\cos\left(n(\theta - k\,z)\right) + b_n(k)\sin\left(n(\theta - k\,z)\right)\right\} \\ B_\theta(r,\theta,z) = -\dfrac{1}{r}\dfrac{\partial \phi_h}{\partial \theta} = B_{ref}(k)\, r_0 \displaystyle\sum_{n=1}^{\infty} n! \left[\frac{2}{n\,k\,r_0}\right]^n \frac{I_n(n\,k\,r)}{r} \left\{a_n(k)\sin\left(n(\theta - k\,z)\right) + b_n(k)\cos\left(n(\theta - k\,z)\right)\right\} \\ B_z(r,\theta,z) = -\dfrac{\partial \phi_h}{\partial z} = B_{ref}(k)\, r_0 \displaystyle\sum_{n=1}^{\infty} (-k)\, n! \left[\frac{2}{n\,k\,r_0}\right]^n I_n(n\,k\,r) \left\{a_n(k)\sin\left(n(\theta - k\,z)\right) + b_n(k)\cos\left(n(\theta - k\,z)\right)\right\} \end{cases} \quad (A1)$$

where $k = 2\pi / L$, L is a twist pitch length. Then, for four helical line currents with dipole symmetry,

helical line current #1 : current +I , radius a, angle ϕ ,
helical line current #2 : current - I , radius a, angle $\pi - \phi$,
helical line current #3 : current - I , radius a, angle $\pi + \phi$,
helical line current #4 : current +I , radius a, angle $-\phi$,

Bref, a_n , b_n are calculated as follows,

A_n=Bref a_n=0 for n=1, 2, 3, 4, ...,
B_n=Bref b_n=0 for n=2, 4, 6, ... ,

and

$$B_n(k) = B_{ref}(k)\, b_n(k) = -\frac{4\mu_0}{\pi} I \frac{1}{2^n(n-1)!\, r_0} (n\,k\,r_0)^n \left(k\,a\,K_{n-1}(n\,k\,a) + K_n(n\,k\,a)\right) \cos n\varphi \qquad (A2)$$

for n=1, 3, 5, ... , ∞.

Then, for many sets of four helical line currents with dipole symmetry,

$$B_n(k) = B_{ref}(k)\, b_n(k) = -\frac{4\mu_0}{\pi} \frac{1}{2^n(n-1)!\, r_0} (n\,k\,r_0)^n \sum_i I_i \left(k\,a_i\,K_{n-1}(n\,k\,a_i) + K_n(n\,k\,a_i)\right) \cos n\varphi_i \qquad (A3)$$

for n=1, 3, 5, ... , ∞.

With the definition of $b_1(k)$ =1 (=constant), $B_{ref}(k) = B_1(k)$. Then, the asymptotic form for the reference field $B_{ref}(k)$, and these helical multipole coefficients $a_n(k)$, $b_n(k)$ as $k \to 0$ ($L \to \infty$) is,

$$\begin{cases} \mathrm{Lim}_{k\to 0}\left[B_{ref}(k)\right] = B_{ref} \\ \mathrm{Lim}_{k\to 0}\left[a_n(k)\right] = a_n \\ \mathrm{Lim}_{k\to 0}\left[b_n(k)\right] = b_n \end{cases} \qquad (A4)$$

That is,

$a_n(k)$ -> a_n (European) = - a_{n-1} (American) : skew multipole coefficient of the 2n-pole
$b_n(k)$ -> b_n (European) = b_{n-1}(American) : normal multipole coefficient of the 2n-pole

Appendix 2. Magnetic Field of 2-dimensional Dipole Coils

The interior magnetic field of 2-dimensional dipole coil with the infinite length is as follows, on the European definition, [3]

$$\begin{cases} B_r(r,\theta) = -\dfrac{\partial\phi}{\partial r} = \dfrac{1}{r}\dfrac{\partial A_z}{\partial\theta} = B_{ref}\displaystyle\sum_{n=1}^{\infty} \left(\frac{r}{r_0}\right)^{n-1}(-a_n \cos n\theta + b_n \sin n\theta) \\ B_\theta(r,\theta) = -\dfrac{1}{r}\dfrac{\partial\phi}{\partial\theta} = -\dfrac{\partial A_z}{\partial r} = B_{ref}\displaystyle\sum_{n=1}^{\infty} \left(\frac{r}{r_0}\right)^{n-1}(b_n \cos n\theta + a_n \sin n\theta) \end{cases} \qquad (A5)$$

Then, the x and y components of field become,

$$\begin{cases} B_x(r,\theta) = B_r(r,\theta)\cos\theta - B_\theta(r,\theta)\sin\theta \\ B_y(r,\theta) = B_r(r,\theta)\sin\theta + B_\theta(r,\theta)\cos\theta \end{cases} \quad (A6)$$

$$\begin{cases} B_x(r,\theta) = B_{ref}\sum_{n=1}^{\infty}\left(\frac{r}{r_0}\right)^{n-1}\left\{-a_n\cos\left[(n-1)\theta\right] + b_n\sin\left[(n-1)\theta\right]\right\} \\ B_y(r,\theta) = B_{ref}\sum_{n=1}^{\infty}\left(\frac{r}{r_0}\right)^{n-1}\left\{a_n\sin\left[(n-1)\theta\right] + b_n\cos\left[(n-1)\theta\right]\right\} \end{cases} \quad (A7)$$

Therefore, on the case with the top-bottom symmetry, $a_n=0$ for n=1, 2, 3, ... , ∞, the y component of field $B_y(x)$ on the x axis becomes,

$$B_y(x)\big|_{y=0} = B_y(r=x,\theta=0) = B_\theta(r=x,\theta=0) = B_{ref}\sum_{n=1}^{\infty} b_n\left(\frac{x}{r_0}\right)^{n-1} = B_{ref}\left(b_1 + b_2\frac{x}{r_0} + b_3\left(\frac{x}{r_0}\right)^2 + \cdots\right) \quad (A8)$$

In addition, for many sets of four line currents with dipole symmetry,

$$B_n = B_{ref}\, b_n = -\frac{2\mu_0}{\pi} r_0^{n-1}\sum_i I_i\, a_i^{-n}\cos n\varphi_i \quad (A9)$$

for n=1, 3, 5, ... , ∞.

References

1) M. Okamura, to be published to Spin Note.

2) T. Tominaka, "Magnetic Field Calculation of Helical Dipole Coils", AGS/RHIC/SN No.24, April 29, (1996).

3) K. -H. Mess, P. Schmüser and S. Wolff , "Superconducting Accelerator Magnets", World Scientific, p.44-53 (1996).

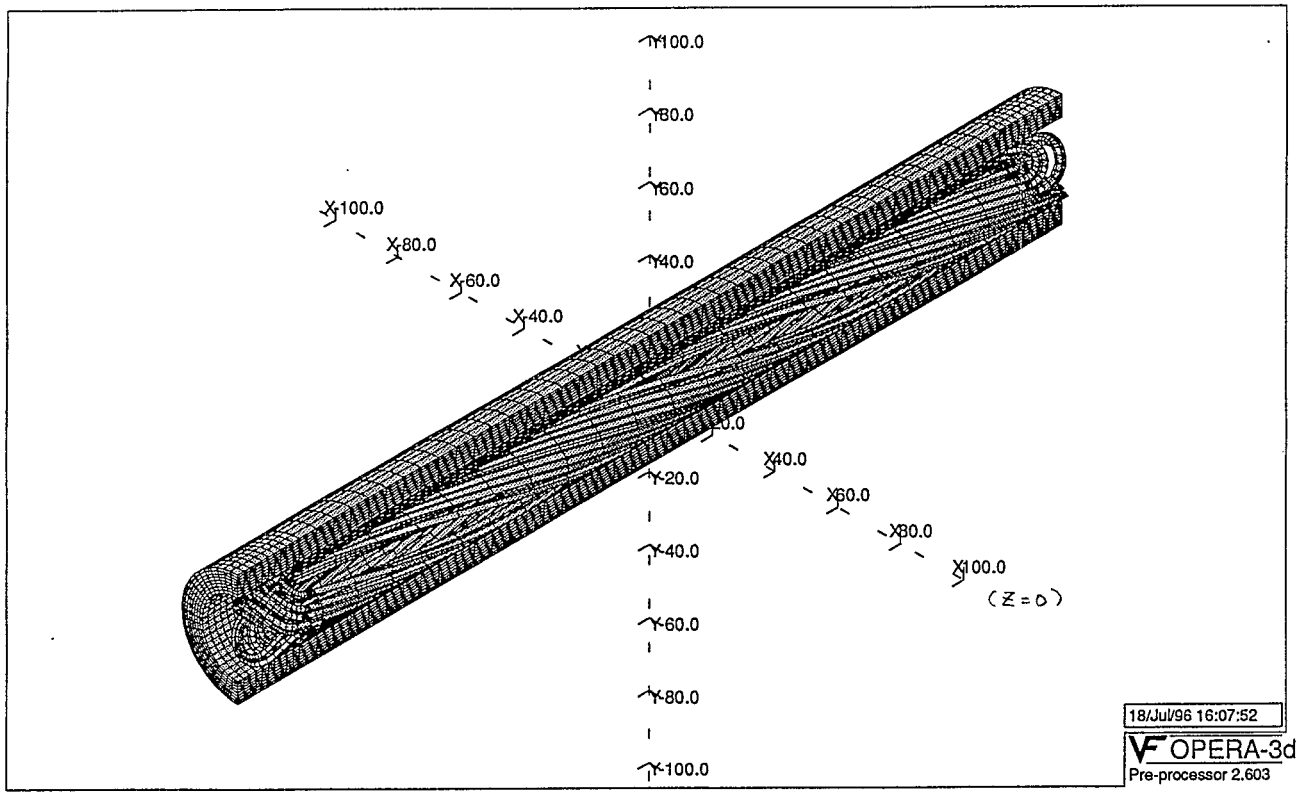

Fig.1 Schematic view of a slotted helical dipole designed in BNL.

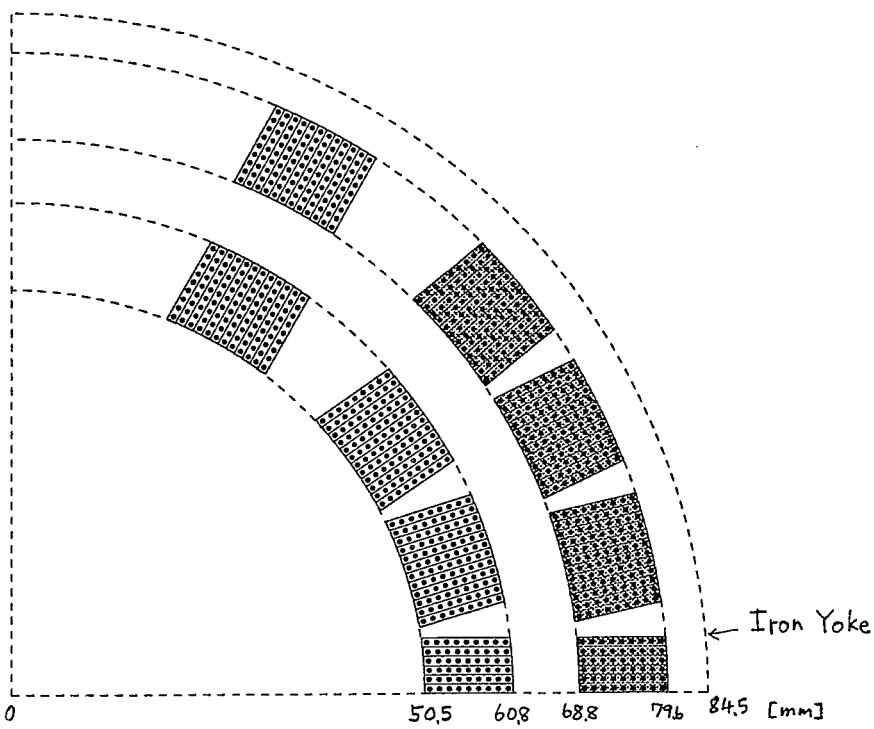

Fig.2 Cross section of a slotted helical dipole optimized at BNL. The current of white region is 290 A, and that of gray region 354.4 A.

Table 1 Helical and 2-dimensional normal multipole coefficients derived from the field distribution with the reference radius r0=30 mm for the cross section shown in Fig.2 without iron yoke.

n (Bref)	b-helix 2.77096 [T]	b-2d 2.71479 [T]
1	1.	1.
3	-0.00186318	-0.00188604
5	0.000265931	0.000263292
7	$-9.96646\ 10^{-6}$	-0.000012757
9	-0.000792894	-0.000842947
11	0.00029096	0.00031248
13	0.0000146582	0.0000158341
15	-0.0000319603	-0.0000349333
17	$4.04886\ 10^{-6}$	$4.46808\ 10^{-6}$
19	$2.38084\ 10^{-6}$	$2.64973\ 10^{-6}$

Table 2 Helical and 2-dimensional normal multipole coefficients derived from the field distribution with the reference radius r0=30 mm for the cross section shown in Fig.2 with iron yoke.

n (Bref)	b-helix 4.49623 [T]	b-2d 4.37827 [T]
1	1.	1.
3	-0.000189721	-0.000166809
5	0.0000398628	0.0000286006
7	-0.0000144962	-0.0000172929
9	-0.000490655	-0.000525023
11	0.000179759	0.000194288
13	$9.02359\ 10^{-6}$	$9.80574\ 10^{-6}$
15	-0.000019701	-0.0000216662
17	$2.49566\ 10^{-6}$	$2.771\ 10^{-6}$
19	$1.46729\ 10^{-6}$	$1.643\ 10^{-6}$

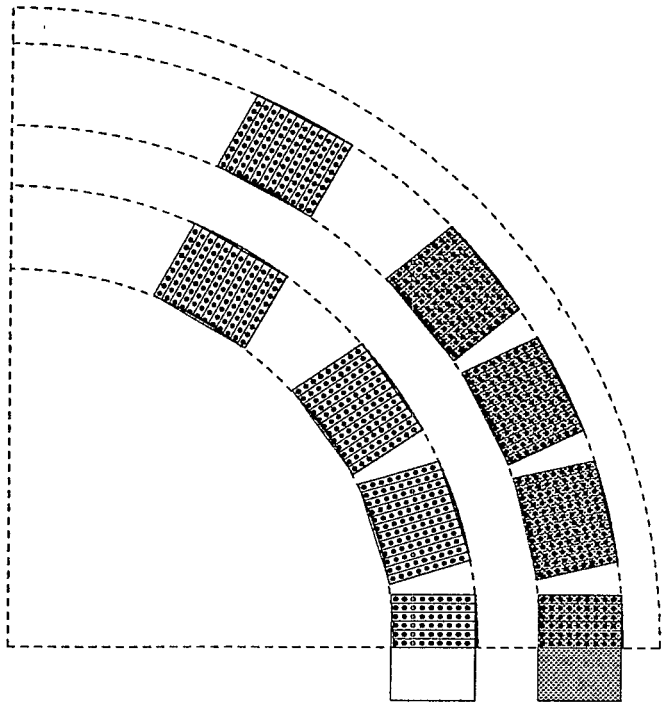

Fig.3 Cross section of a slotted helical dipole deformed for machining from the optimized one.

Table 3 Helical and 2-dimensional normal multipole coefficients derived from the field distribution with the reference radius r0=30 mm for the cross section shown in Fig.3 without iron yoke.

n (Bref)	b-helix 2.78725 [T]	b-2d 2.73119 [T]
1	1.	1.
3	-0.00192387	-0.00194781
5	0.000282415	0.000280139
7	$-9.44077\ 10^{-6}$	-0.0000122488
9	-0.000838267	-0.000890559
11	0.000312108	0.000334906
13	0.0000160162	0.0000172859
15	-0.0000356478	-0.0000389179
17	$4.64905\ 10^{-6}$	$5.1227\ 10^{-6}$
19	$2.86908\ 10^{-6}$	$3.18685\ 10^{-6}$

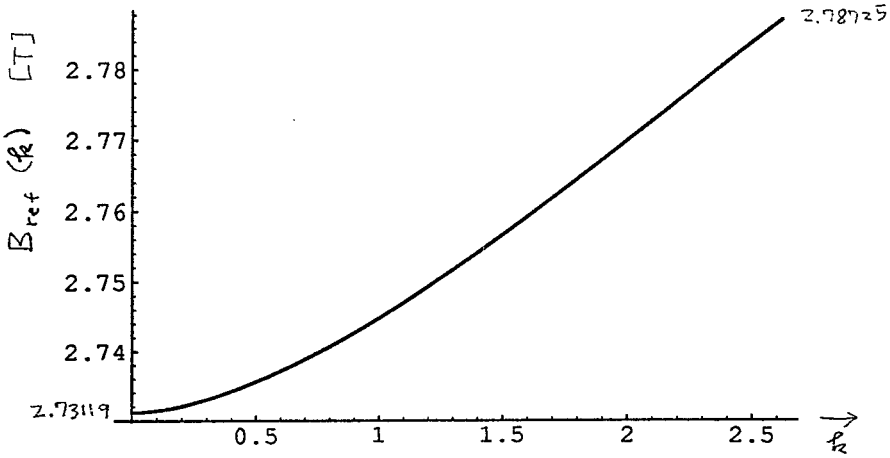

Fig.4 The twist dependence of the reference field Bref(k).

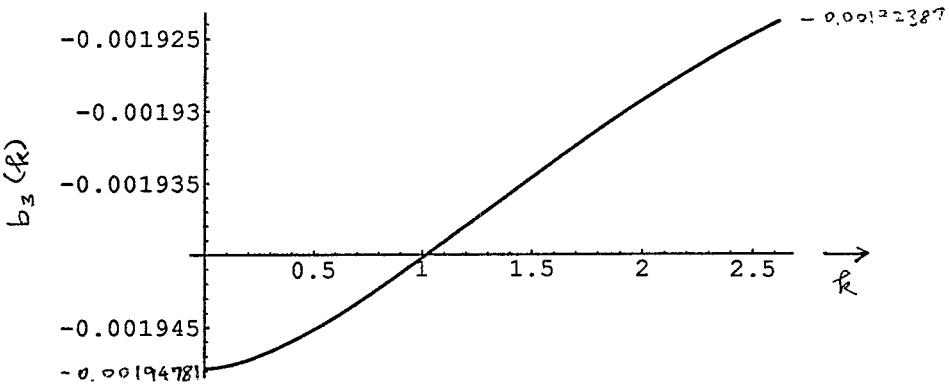

Fig.5 The twist dependence of the sextuple coefficient b3(k).

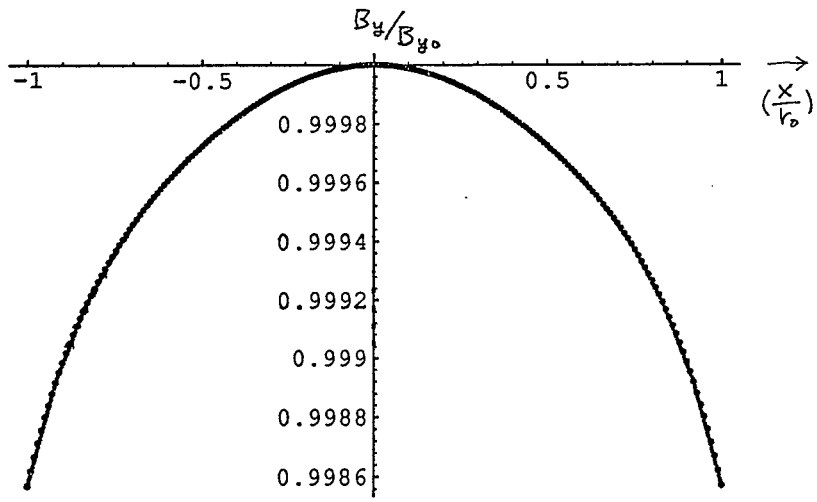

Fig.6 The field distribution of By on the x axis.

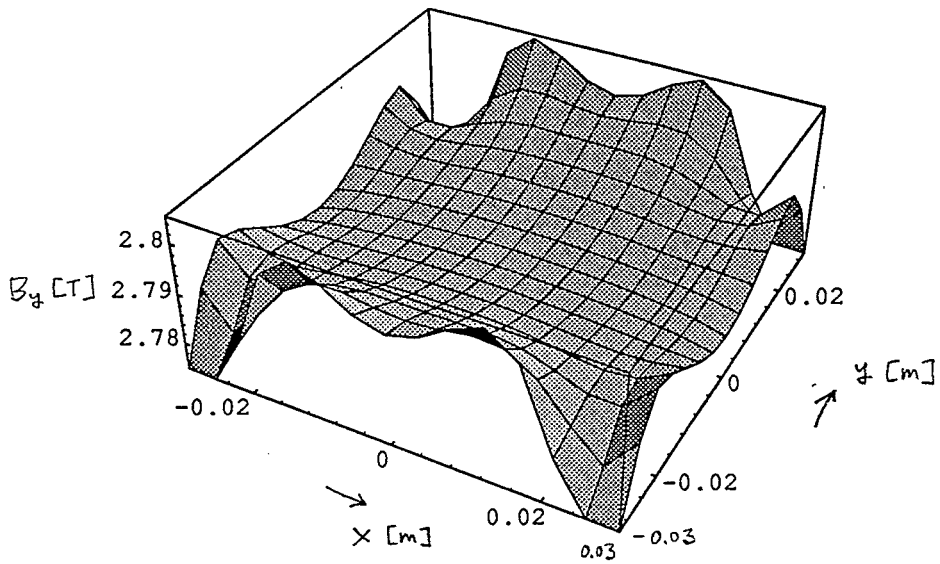

Fig.7 The field distribution of By for the cross section shown in Fig.3 without iron yoke.

Table 4 Helical and 2-dimensional normal multipole coefficients derived from the field distribution with the reference radius r0=30 mm for the cross section shown in Fig.2 with iron yoke.

n	b-helix	b-2d
(Bref)	4.50281 [T]	4.38495 [T]
1	1.	1.
3	-0.000246234	-0.000224954
5	0.0000542499	0.0000435128
7	-0.0000138513	-0.0000166319
9	-0.000520782	-0.000556905
11	0.00019361	0.000209095
13	$9.90482\ 10^{-6}$	0.0000107552
15	-0.00002207	-0.0000242451
17	$2.87813\ 10^{-6}$	$3.19117\ 10^{-6}$
19	$1.77598\ 10^{-6}$	$1.98496\ 10^{-6}$

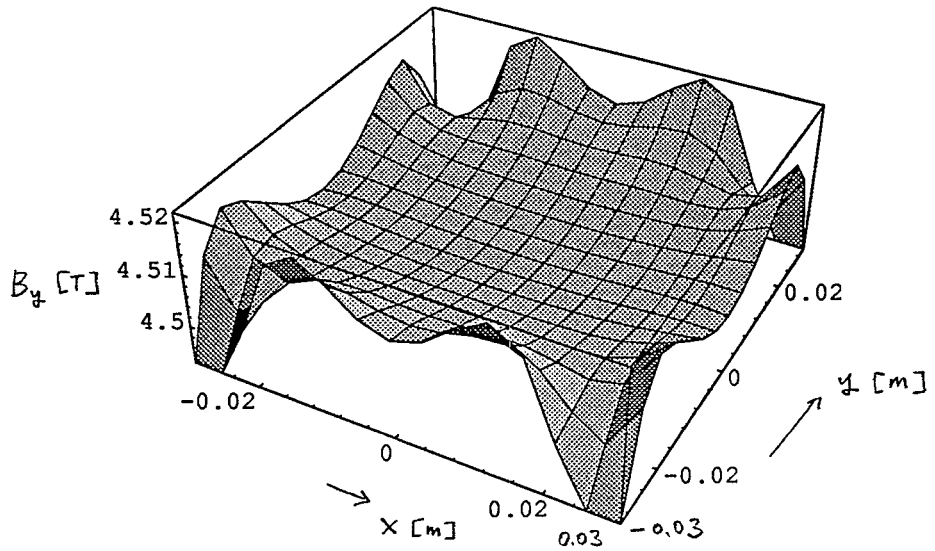

Fig.8 The field distribution of By for the cross section shown in Fig.3 with iron yoke.

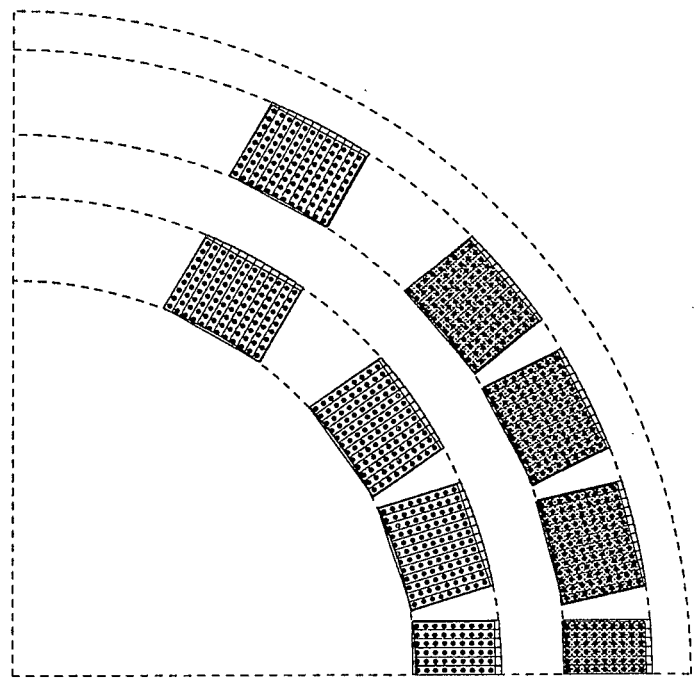

Fig.9 Cross section of a slotted helical dipole, obtained from the input data for OPERA-3d.

Table 5 Helical and 2-dimesional normal multipole coefficients derived from the field distribution with the reference radius r0=30 mm for the cross section shown in Fig.3 without iron yoke.

n (Bref)	b-helix 2.78779 [T]	b-2d 2.73175 [T]
1	1.	1.
3	-0.00202305	-0.00205003
5	0.000326291	0.000326187
7	-0.0000102877	-0.0000132087
9	-0.000833307	-0.000885304
11	0.000318336	0.000341562
13	0.0000154094	0.0000166236
15	-0.000035921	-0.0000392179
17	$5.17271\ 10^{-6}$	$5.69637\ 10^{-6}$
19	$3.09876\ 10^{-6}$	$3.44077\ 10^{-6}$

Table 6 Helical normal multipole coefficients derived from Br, Btheta, Bz distribution on the circle of radius r=30 mm at z=0, calculated with OPERA-3d

n (Bref)	bn-r 2.7922 [T]	bn-theta 2.7922 [T]	bn-z 2.7922 [T]
1	0.999905	1.00007	1.00252
3	-0.00221742	-0.00222662	-0.0023024
5	0.000279781	0.000289925	0.00027661
7	-0.0000240421	$-7.18715\ 10^{-6}$	-0.0000102329
9	-0.000851626	-0.000829641	-0.0008293
11	0.000326181	0.00031585	0.000319438
13	0.0000122363	$4.54053\ 10^{-6}$	$2.13571\ 10^{-6}$
15	-0.000030323	-0.0000533146	-0.0000550198
17	$-4.7188\ 10^{-6}$	$6.84087\ 10^{-6}$	$7.83723\ 10^{-6}$
19	-0.0000164482	-0.0000114868	$-7.91002\ 10^{-6}$

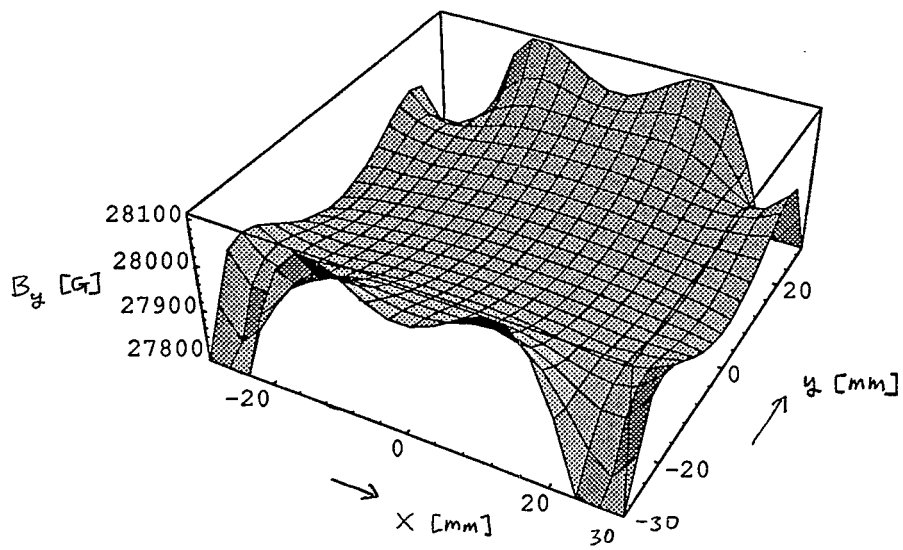

Fig.10 The field distribution of By for the cross section shown in Fig.9 without iron yoke, calculated with OPERA-3d